

Shared receptors in axon guidance: SAX-3/Robo signals via UNC-34/Enabled and a Netrin-independent UNC-40/DCC function

Timothy W. Yu¹, Joe C. Hao^{1,2}, Wendell Lim³, Marc Tessier-Lavigne² and Cornelia I. Bargmann¹

¹ Howard Hughes Medical Institute, Program in Neuroscience, Department of Anatomy and of Biochemistry and Biophysics, The University of California, San Francisco, California 94143, USA

² Present address: Department of Biological Sciences, Howard Hughes Medical Institute, 371 Serra Hall, Stanford University, Stanford, California 94305, USA

³ Department of Molecular and Cellular Pharmacology, The University of California, San Francisco, California 94143, USA

Correspondence should be addressed to C.I.B. (cori@itsa.ucsf.edu)

Published online 15 October 2002; doi:10.1038/nn956

The *C. elegans* SAX-3/Robo receptor acts in anterior–posterior, dorsal–ventral and midline guidance decisions. Here we show that SAX-3 signaling involves the *C. elegans* Enabled protein UNC-34 and an unexpected Netrin-independent function of the Netrin receptor UNC-40/DCC. Genetic interactions with gain- and loss-of-function mutations suggest that *unc-34* and *unc-40* act together with *sax-3* in several guidance decisions, but the *C. elegans* Netrin gene *unc-6* does not act in the same genetic pathways. Within the migrating axon, *sax-3*, *unc-34* and *unc-40* all act cell-autonomously. Our results support a role for UNC-34/Enabled proteins in SAX-3-mediated repulsion, and show that UNC-40/DCC can potentiate SAX-3/Robo signaling via a mechanism that may involve direct binding of the two guidance receptors. A combinatorial logic dictates alternative functions for UNC-40/DCC, which can act in attraction to UNC-6/Netrin, repulsion from Netrin (with UNC-5), or repulsion from Slit (with SAX-3).

Growth cones of developing neurons navigate through their environments by responding to attractive and repulsive guidance cues¹. Several conserved families of ligands and receptors participate in axon guidance, including UNC-6/Netrin and its receptors UNC-40/DCC/Frazzled and UNC-5, Slit and its receptor Robo/SAX-3, Ephrins and the Eph receptors, and Semaphorins and their receptors Neuropilin and Plexin^{2–6}. Although the cytoplasmic domains of most guidance receptors lack obvious similarity to one another, these domains define the guidance functions of the receptors. Thus, when the cytoplasmic sequences of UNC-40/DCC/Frazzled and SAX-3/Robo are fused to heterologous ligand-binding domains, they can drive axon attraction or repulsion, respectively^{7,8}.

The function of a particular guidance receptor can vary depending on the cell and its environment. For example, UNC-40/DCC is required for attraction to UNC-6/Netrin, but some cells that express UNC-40 are not attracted to Netrin, suggesting that UNC-40 requires additional cofactors to mediate attractive guidance⁹. In addition to its role in attraction, UNC-40 also potentiates repulsion from Netrin mediated by the UNC-5 receptor^{10,11}. This potentiation occurs through a direct interaction between the UNC-40 and UNC-5 cytoplasmic domains that is stimulated by Netrin binding¹². There are also Netrin-independent functions of UNC-40 in cell and axon migration^{13–16}.

We are studying mechanisms of axon repulsion mediated by *C. elegans sax-3*, a member of the Robo family of guidance receptors. The nematode, fly and human SAX-3/Robo proteins are

transmembrane receptors with five immunoglobulin domains, three fibronectin type III domains, and cytoplasmic domains from 377 to 733 amino acids in size^{17,18}. *Drosophila Robo* and *C. elegans sax-3* mutants have defects in repulsion of axons from the ventral midline^{17–21}. In *Drosophila*, the secreted Robo ligand Slit is expressed at the midline, where it acts to repel Robo-expressing axons²². *C. elegans sax-3* mutants also have defects in long-range cell migrations, in the formation of the nerve ring in the head, and in ventral axon guidance in the body²³. A *C. elegans* Slit homolog, *slt-1*, is a ligand for *sax-3* in several guidance decisions²⁴. Vertebrate Robos and Slits act in repulsion from midline structures and at other locations^{25–29}.

Genetic screens in *C. elegans* and *Drosophila* have led to the identification of several genes that are candidate downstream components of axon guidance signaling pathways^{30–32}. One of these genes, *enabled*, was identified in *Drosophila* as a genetic suppressor of lethal mutations in the tyrosine kinase *abl*³³; subsequent analysis of *ena* mutants revealed axon guidance defects in the *Drosophila* nervous system³⁴. Dose-dependent interactions between *ena*, *abl*, and genes for receptor tyrosine phosphatases (RPTPs) suggested that these proteins act in a common regulatory pathway for axon guidance³⁵.

We show here that the *C. elegans* Enabled protein UNC-34 is a mediator of SAX-3 signaling in repulsive guidance from SLT-1. Robo and Enabled also act together in *Drosophila* midline guidance³⁶. We also report the unexpected finding that SAX-3

Table 1. Neuronal guidance in wild type, *sax-3* mutants and *unc-34* mutants.

	wild type	<i>sax-3</i>	<i>unc-34</i>
Cell migration			
CAN cells	posterior migration	stop short¹	stop short²
Ventral nerve cord			
PVQ interneurons	do not cross midline	cross midline³	cross midline
<i>glr-1</i> interneurons	ventral	lateral³	lateral⁴
HSN motor neurons	anterior to head	anterior to head	terminate⁵
Dorsal/ventral guidance			
AVM axon	ventral guidance	guidance defect¹	guidance defect
VD and DD axons	dorsal guidance	dorsal guidance	guidance defect⁵
Nerve ring			
<i>ceh-23</i> sensory neurons	nerve ring	anterior misguidance¹	nerve ring
<i>glr-1</i> interneurons	nerve ring	anterior misguidance¹	nerve ring

¹Zallen et al., 1999. ²Forrester and Garriga, 1997. ³Zallen et al., 1998. ⁴S. Clark and C.I.B., unpub. observ. ⁵McIntire et al., 1992. Other observations are from the present paper. Boldface denotes mutant phenotypes.

function is potentiated by a Netrin-independent function of the Netrin receptor UNC-40. Our results suggest that SAX-3, UNC-34 and UNC-40 may interact in complexes that drive repulsive guidance.

RESULTS

Overlap in *sax-3/Robo* and *unc-34/Ena* phenotypes

A conserved proline-rich motif in the cytoplasmic domains of *C. elegans* SAX-3, *Drosophila* Robo1 and human Robo1 receptors resembles a consensus binding site for EVH1 domains, domains characteristic of Enabled proteins and their family members¹⁸. This motif, designated CC2, has a core of seven conserved prolines flanked by hydrophobic amino acids (in SAX-3, FIPP-SNP). The evidence implicating Enabled in *Drosophila* axon guidance and the presence of this recognition site led us to study

interactions between SAX-3 and *C. elegans* EVH1 domain-containing proteins.

C. elegans has three predicted EVH1 domain proteins: a single Enabled homolog on chromosome V (overlapping the predicted gene Y50D4C.1; Methods) and two other EVH1-containing proteins on chromosome III (B0280.2) and IV (C07G1.4). To ask whether the *C. elegans* Enabled protein affects cell and axon migrations, we disrupted its function using double-stranded RNA-mediated interference³⁷. RNAi of Y50D4C.1 in wild-type *C. elegans* resulted in cell migration defects in the CAN neuron, a withered tail phenotype, and an uncoordinated (Unc) phenotype (data not shown). Similar CAN migration and withered tail phenotypes are observed in *sax-3* mutants. These defects are also observed in *unc-34* mutants, which map to the same region of chromosome V as Y50D4C.1, suggesting that Y50D4C.1 might correspond to *unc-34*. Indeed, *unc-34* encodes the *C. elegans*

Enabled homolog and the allele *unc-34(gm104)* has been identified as a molecular null allele (M. Dell and G. Garriga, pers. comm.).

To ask whether *unc-34* has a role in *sax-3* signaling, we first compared the mutant phenotypes of *sax-3* and *unc-34* mutants. *sax-3* and *unc-34* mutants share a highly penetrant defect in the posterior migration of the CAN neurons (Table 1)^{17,38,39}. We observed that they shared several other defects that were not previously described. These include inappropriate midline crossing by the two PVQ axons (37% penetrance in *unc-34(gm104)*, *n* = 114; 55% in *sax-3(ky123)*¹⁷, *n* = 70), inappropriate lateral axon migrations of *glr-1*-expressing interneurons (S. G. Clark and C.I.B., unpub. data), and defects in ventral migration of the AVM sensory axons²³ (Fig. 1a–l; Table 1). However, other phenotypes of *sax-3* and *unc-34* mutants were not identical: only

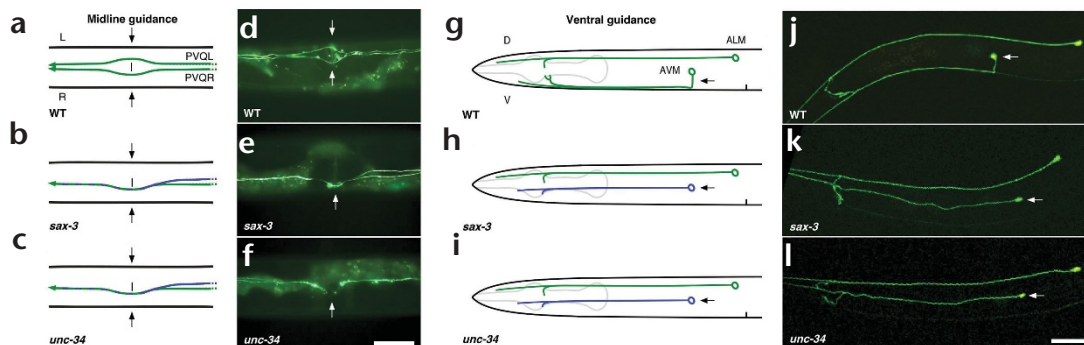
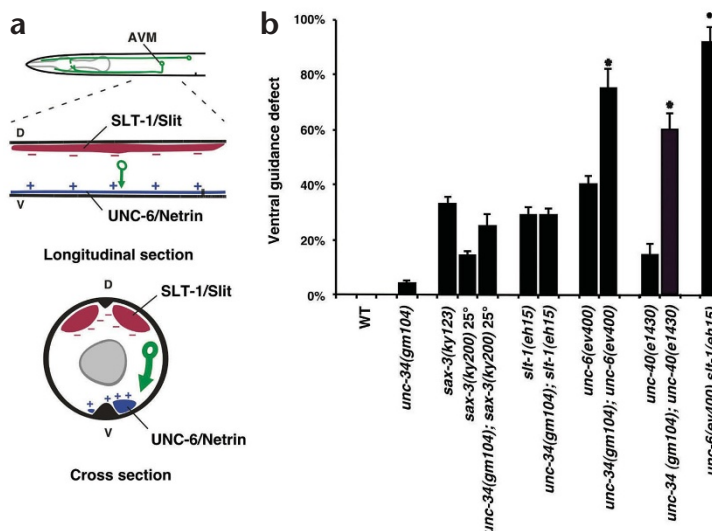


Fig. 1. *unc-34* and *sax-3* mutants share axon guidance phenotypes at the ventral midline and in ventral guidance. (a–f) Ventral views of ventral cord axons expressing *sra-6::gfp* in wild-type (a, d), *sax-3* (b, e) or *unc-34* (c, f) backgrounds. (a, d) In wild-type animals, axons from the two PVQ interneurons extend in the ventral nerve cord where they are restricted to the ipsilateral nerve cord. (b, e) In a *sax-3(ky123)* mutant animal, the PVQ axons cross the midline. Here both PVQ axons run on the right side of the vulva (arrows). (c, f) In an *unc-34(gm104)* mutant animal, the PVQ axons also cross the midline (arrows). (g–l) Ventral guidance phenotypes visualized by *mec-4::gfp* in wild-type (g, j), *sax-3* (h, k) or *unc-34* (i, l) mutant backgrounds. (g, j) In wild-type animals, AVM (arrow) grows ventrally to the ventral cord, and then extends anteriorly to the nerve ring. (h, k) In *sax-3* mutant animals, AVM has ventral guidance defects. Shown is a *sax-3(ky123)* animal in which AVM fails to grow ventrally and extends directly anteriorly. (i, l) *unc-34* mutants also have ventral guidance defects in AVM. Anterior is left in all panels. Scale bars, 20 μm.

Fig. 2. *unc-34* double mutant analysis in AVM ventral guidance. (a) Organization of guidance cues for AVM ventral guidance in *C. elegans*. SLT-1 is expressed dorsally in muscle (red), whereas UNC-6 is expressed ventrally in the ventral nerve cord (blue). AVM (green) expresses both SAX-3 and UNC-40 guidance receptors. (b) Quantitation of ventral guidance defects in *sax-3*, *slt-1*, *unc-6*, *unc-40* and *unc-34* single and double mutants. * Defects greater than those of the *unc-6* or *unc-40* single mutant ($P < 0.01$).



sax-3 mutants have anteriorly misrouted sensory axons in the nerve ring¹⁷, and only *unc-34* mutants exhibit misguidance of motor axons and premature termination of axons in the ventral nerve cord³⁹. We conclude that *sax-3* and *unc-34* mutants share some, but not all, axon and cell migration defects.

***sax-3* and *unc-34* act in a common genetic pathway**

We used genetic criteria to test the involvement of *unc-34* in *sax-3* signaling. If two genes act exclusively in the same pathway, a double mutant should be similar to the strongest single null mutant. The phenotype of the strong *sax-3(ky123)* allele, which lacks the start and signal sequence of SAX-3, served as the presumed *sax-3* null phenotype. A strong *sax-3* phenotype is also caused by the *sax-3(ky200ts)* mutant at 25°C. The strong *slt-1(eh15)* allele, which truncates SLT-1 near the N terminus, was used to inactivate SLT-1 function²⁴, and the *unc-34(gm104)* null allele was used.

We examined *sax-3*, *slt-1* and *unc-34* in detail for the ventral guidance of the AVM mechanosensory neuron, the best-characterized *sax-3*-dependent guidance decision. The AVM cell body lies on the lateral body wall; at the end of the first larval stage (L1), its axon grows ventrally to the ventral nerve cord, where it turns anteriorly and extends to the nerve ring (Fig. 1g and j; Fig. 2a)⁴⁰. The initial ventral guidance of the AVM axon is mediated in part by repulsion from SLT-1, which is expressed by dorsal muscles. In AVM, *sax-3* is required for repulsion from SLT-1²³; in strong *sax-3* or *slt-1* mutants, 30–40% of AVM neurons fail in the initial ventral component of their trajectory and instead take an anterior path appropriate for the second part of their trajectory (Fig. 1h and k; Fig. 2b). On their own, *unc-34* mutants had a mild defect in AVM ventral guidance (Fig. 1i and l; Fig. 2b). AVM defects in *unc-34*; *slt-1* double mutants were

similar to those of strong *slt-1* single mutants, and a similar result was observed for *unc-34*; *sax-3(ky200)* (Fig. 2b). (The *unc-34*; *sax-3(ky123)* double mutants were not viable, precluding analysis of AVM axon guidance.) These results are consistent with a role for *unc-34* in the *slt-1*/*sax-3* guidance decision.

A second test for similar functions of *sax-3* and *unc-34* is to examine their effects when mutations are combined with mutations in an independent guidance pathway. Netrin/*unc-6* and *slt-1* guidance systems act in parallel to direct AVM ventral guidance: AVM is simultaneously repelled by dorsal SLT-1 and attracted to ventral UNC-6^{24,41}. In the strong *unc-6(ev400)* allele, 40% of AVM axons fail to grow ventrally¹⁴ (Fig. 2b). The defect in *unc-6 slt-1* double mutants is enhanced to over 90%, suggesting a loss of all dorsal–ventral guidance information (Fig. 2b)²⁴. If *unc-34* acts specifically in the *slt-1* pathway, *unc-34* mutants should act like *slt-1* mutants to enhance the AVM ventral guidance defects of null mutants in *unc-6*. Indeed, the ventral guidance defects of *unc-34*; *unc-6* mutants were much more severe than those of single mutants (Fig. 2b). Similar synergistic enhancement was observed in double mutants between *unc-34* and the Netrin receptor *unc-40*. Because the *unc-34* mutation has little effect on AVM on its own, but has a very strong effect in a genetic background

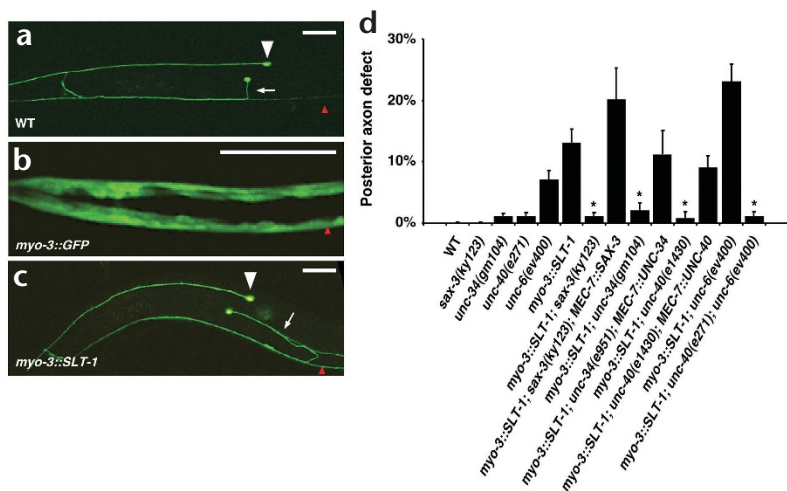
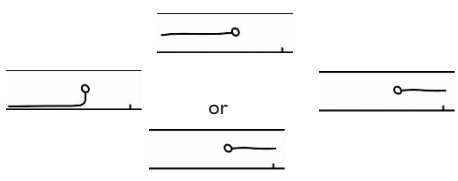


Fig. 3. Suppression of Slit gain-of-function phenotypes by *unc-34* and *unc-40*. (a) A wild-type ventral AVM axon projection (arrow) visualized with *mec-4:gfp*. ALM (white arrowhead) is also visible with this marker. Position of the vulva (red arrowhead) is shown. (b) Expression pattern of the *myo-3* promoter, as visualized by GFP. The *myo-3* promoter drives expression in dorsal and ventral body wall muscle cells. Position of the vulva (red arrowhead) is shown for comparison. (c) Posteriorly directed AVM axon (arrow) caused by misexpression of SLT-1 under the *myo-3* promoter, with positions of ALM (white arrowhead) and the vulva (red arrowhead) shown for reference. (d) Quantitation of posterior axon phenotypes of an integrated *myo-3::SLT-1* transgene (*kyls218*) in a variety of genetic backgrounds. Data shown \pm s.e.m. *Strains that are significantly suppressed compared to *myo-3::SLT-1* alone ($P < 0.01$). Scale bars, 20 μ m.



Table 2. Suppression of *myo-3:SLT-1* gain-of-function A–P phenotype by *sax-3*, *unc-34* and *unc-40*.



Genotype	Percent wild type	Percent anterior or posterior axons (D–V guidance)	Percent posterior axons (A–P guidance)	n
wild type	100	0	0	>300
<i>sax-3(ky123)</i>	67	33	0	383
<i>unc-34(gm104)</i>	97	3	1	252
<i>unc-40(e271)</i>	82	18	1	186
<i>unc-6(ev400)</i>	60	40	7	275
<i>kyls218(myo-3:SLT-1)</i>	68	32	13	213
<i>kyls218; sax-3(ky123)</i>	61	39	1*	223
<i>kyls218; sax-3(ky123); mec-7:SAX-3</i>	64	36	20	76
<i>kyls218; unc-34(gm104)</i>	75	25	3*	330
<i>kyls218; unc-34(e951)</i>	60	40	4*	167
<i>kyls218; unc-34(e951); mec-7:UNC-34</i>	60	40	11	154
<i>kyls223(myo-3:SLT-1)</i>	66	34	14	658
<i>kyls223; unc-34(gm104)</i>	76	24	1*	146
<i>kyls218; unc-40(e271)</i>	24	72	1*	139
<i>kyls218; unc-40(e1430)</i>	39	61	1*	166
<i>kyls218; unc-40(e1430); mec-7:UNC-40</i>	47	53	9	181
<i>kyls213(myo-3:SLT-1)</i>	63	37	9	225
<i>kyls213; unc-40(e271)</i>	28	72	0	39
<i>kyls218; unc-6(ev400)</i>	10	90	23	203
<i>kyls218; unc-40(e1430); unc-6(ev400)</i>	15	85	1*	133

Axons that fail to grow ventrally are classified as D–V guidance defective, and include both anterior and posteriorly guided axons. Asterisks denote double mutants that were significantly suppressed compared to *myo-3:SLT-1* alone ($P < 0.01$).

that relies entirely on *slt-1/sax-3* signaling, these results place *unc-34* in the Slit pathway for AVM ventral guidance.

Additional evidence for a role of *unc-34* in SAX-3/Robo signaling was provided by its ability to suppress a gain-of-function of the *sax-3* pathway. SLT-1 is normally expressed in dorsal muscles. Ubiquitous muscle expression of SLT-1 under the *myo-3* promoter causes both dorsal–ventral defects and anterior–posterior defects in AVM axon guidance, whereas loss-of-function of *sax-3* or *slt-1* causes only dorsal–ventral defects in AVM (Fig. 3)²⁴. The anterior–posterior defects caused by *myo-3:SLT-1* are diagnostic of overactivated SAX-3/SLT-1 signaling, and provide a distinguishable gain-of-function phenotype for epistasis analysis. *sax-3* loss-of-function mutations are strong suppressors of the anterior–posterior defect of *myo-3:SLT-1*, as

expected because loss of a receptor should suppress the effects of excess ligand (Fig. 3d)²⁴. Expression of *sax-3* within AVM using a *mec-7:SAX-3* transgene restored the *myo-3:SLT-1* posterior defect, indicating that *sax-3* acts cell-autonomously in AVM (Fig. 3d; Table 2).

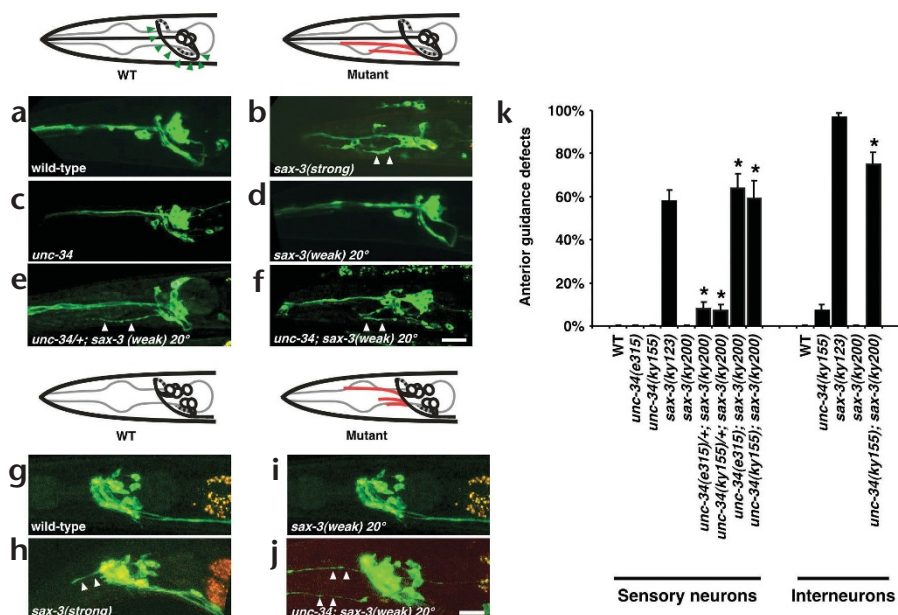
Posterior AVM defects of *myo-3:SLT-1* animals were also suppressed by mutations in *unc-34* (Fig. 3d; Table 2). This epistasis result suggests that *unc-34* acts with *sax-3* downstream of *slt-1*. To ask whether this suppression reflected a function for UNC-34 within the AVM neuron, we isolated a full-length UNC-34 cDNA using RT-PCR. Expression of this *unc-34* cDNA in AVM caused reappearance of posterior guidance defects (Fig. 3d; Table 2), demonstrating that *unc-34* acts cell autonomously to potentiate *slt-1/sax-3* signaling.

The shared CAN migration, midline guidance, and AVM guidance phenotypes of *sax-3* and *unc-34* contrast with the situation in the nerve ring, where *sax-3* and *unc-34* have different phenotypes. Sensory axons exit the nerve ring to take abnormal anterior trajectories in strong *sax-3* mutants such as *sax-3(ky123)*, but not in *sax-3(ky200)* at 20°C or in *unc-34* null mutants (Fig. 4a–d). In a genetic background sensitized by weak mutations in one gene, mutation of a second gene in the pathway can synergize to yield a stronger phenotype. Removing a single copy of *unc-34* in a *sax-3(ky200)* background at 20°C caused anterior sensory axon defects (Fig. 4e). Removing both copies of *unc-34* in a *sax-3(ky200)* background had an even stronger effect, resulting in a defect that was comparable to that of *sax-3* null mutants (Fig. 4f). Similar synergistic interactions were observed in interneuron axons in the nerve ring observed with the marker *glr-1:GFP*. *unc-34* and *sax-3(ky200)* at 20°C had mild anterior axon defects, which were strongly enhanced toward the *sax-3* null phenotype in *unc-34; sax-3(ky200)* double mutants at 20°C (Fig. 4g–k). These results demonstrate that UNC-34 contributes to nerve ring axon guidance, a role not evident from analysis of *unc-34* mutants alone. They therefore reveal another function shared by *sax-3* and *unc-34*, and support the model that *unc-34* and *sax-3* function in a common guidance pathway.

***unc-40* has a Netrin-independent signaling role**

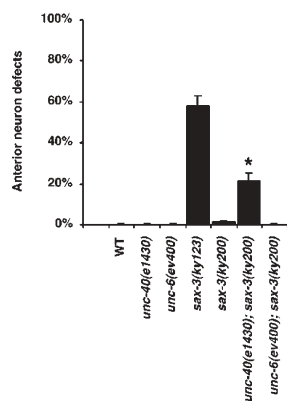
To seek additional components of the *sax-3* guidance pathway, we examined the functions of other axon guidance genes using the genetic assays described above. Surprisingly, we observed that

Fig. 4. Genetic interactions between *sax-3* and *unc-34* in the nerve ring. Phenotypes of sensory axons (a–f), as visualized with the *ceh-23:gfp* marker, and interneurons (g–j), as visualized with the *glr-1:gfp* marker. (a) Wild-type nerve ring, in which sensory axons extend ventrally from their cell bodies into the nerve ring (green arrowheads). Anterior processes are sensory dendrites. (b) *sax-3(ky123)*, a strong loss-of-function mutant. Nearly all axons (schematic, red axons) travel anteriorly beyond the normal confines of the ring. (c) *unc-34* animals have no axon guidance defects in the nerve ring (although some axons terminate prematurely within the nerve ring). (d) *sax-3(ky200ts)* at the permissive temperature (20°C). Sensory axons are normal. (e) *sax-3(ky200ts) unc-34/+* at the permissive temperature (20°C). One axon grows anteriorly beyond the confines of the nerve ring. (f) *sax-3(ky200ts) unc-34* at the permissive temperature (20°C). A highly disorganized, anterior nerve ring reminiscent of the strong *sax-3* phenotype. (g) Wild-type animals, in which interneuron axons extend within the nerve ring en route to or from the ventral cord. (h) *sax-3(ky123)* animal. *glr-1*-expressing axons leave the nerve ring to travel anteriorly. (i) *sax-3(ky200ts)* at the permissive temperature (20°C). Interneuron axons are normal. (j) *sax-3(ky200ts) unc-34* at the permissive temperature (20°C), with anterior axon phenotype reminiscent of the strong *sax-3* phenotype. (k) Quantitation of anterior guidance defects in the nerve ring. *Double mutants that are enhanced compared to *sax-3(ky200ts)* alone ($P < 0.01$). Data shown \pm s.e.m. for proportions. White arrowheads, aberrant trajectories. Scale bars, 20 μ m.



mutations in the Netrin receptor *unc-40* strongly suppressed anterior–posterior AVM defects in the *myo-3:SLT-1* strain (Fig. 3d; Table 2). Because the anterior–posterior defects are a specific result of SLT-1 misexpression, this result suggested that the gain-of-function SLT-1 phenotype requires the UNC-40 guidance receptor in addition to the SAX-3 guidance receptor. Expression of *unc-40* in touch neurons under the *mec-7* promoter was sufficient to restore posterior AVM axons to *unc-40; myo-3:SLT-1* animals (Fig. 3d; Table 2). These results indicate that *unc-40* acts cell-autonomously in AVM to modulate SLT-1 responses.

Mutations in *unc-6/Netrin* did not suppress the gain-of-function SLT-1 phenotype, suggesting that UNC-40 does not act as a Netrin receptor in this context (Fig. 3d; Table 2). In *Drosophila*, neurons expressing the *unc-40* homolog *frazzled* can bind Netrin and present it to developing axons⁴². If UNC-40 binds and redistributes the UNC-6 protein, mutations in *unc-40* could



cause *unc-6*-dependent defects in pathfinding. To ask if the suppression of *myo-3:SLT-1* by *unc-40* was secondary to a redistribution of UNC-6, we examined an *unc-40; unc-6 myo-3:SLT-1* triple mutant. The triple mutant phenotype was identical to that of *unc-40; myo-3:SLT-1* (Fig. 3d). Thus the ability to suppress *myo-3:SLT-1* is not due to UNC-6 redistribution and is an *unc-6*-independent function of *unc-40*.

To test whether *unc-40* is involved in other *sax-3*-dependent guidance pathways, we examined the enhancement of nerve ring axon guidance defects in animals harboring the weak *sax-3(ky200)* allele. *unc-40* mutants did not have anterior guidance defects in the nerve ring. However, *unc-40; sax-3(ky200)* mutants at 20°C showed a substantial enhancement of anterior nerve ring phenotypes compared to *sax-3(ky200)* alone, yielding a phenotype similar to that of strong *sax-3* mutants (Fig. 5). No enhancement was observed in *unc-6(ev400) sax-3(ky200)* double mutants (Fig. 5). Thus, the nerve ring defect, like the *myo-3:SLT-1* defect, results from a Netrin-independent function of *unc-40*.

In summary, like *unc-34/Enabled* mutations, *unc-40/DCC* mutations suppress a SLT-1 gain-of-function defect in AVM guidance and enhanced weak *sax-3* loss-of-function defects in the nerve ring. Neither of these *unc-40* functions was shared with *unc-6*.

Fig. 5. Genetic interactions between *sax-3* and *unc-40* in the nerve ring. Like *unc-34*, *unc-40* mutations have no anterior axon guidance defects in the nerve ring on their own; however, a contribution of *unc-40* to anterior nerve ring guidance is revealed in a sensitized *sax-3(ky200ts)* background. *Double mutants that are enhanced compared to *sax-3(ky200ts)* alone ($P < 0.01$). Data shown \pm s.e.m.

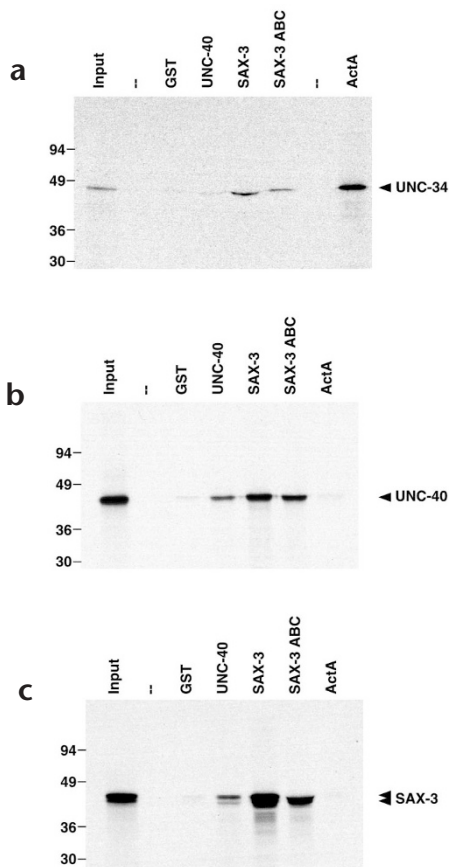


Fig. 6. SAX-3, UNC-34 and UNC-40 proteins can associate *in vitro*. (a) UNC-34 associates *in vitro* with the SAX-3 cytoplasmic domain, but not with either GST alone or the UNC-40 cytoplasmic domain. UNC-34 also associates with the *Listeria* protein ActA. Arrow, band corresponding to full-length ³⁵S-labeled UNC-34 probe. (b) The UNC-40 cytoplasmic domain associates with itself and with the SAX-3 cytoplasmic domain *in vitro*, but not with GST alone or with *Listeria* ActA protein. Arrow, band corresponding to ³⁵S-labeled UNC-40 cytoplasmic domain probe. (c) The SAX-3 cytoplasmic domain associates with itself and with the UNC-40 cytoplasmic domain *in vitro*, but not with GST alone or with *Listeria* ActA protein. Double arrow, bands corresponding to ³⁵S-labeled SAX-3 cytoplasmic domain probe. Input, 1/20th of input probe; –, blank, GST, GST alone; UNC-40, GST fused to the UNC-40 cytoplasmic domain (amino acids 1106–1415); SAX-3, GST fused to the SAX-3 cytoplasmic domain (amino acids 898–1273); SAX-3 ABC, GST fused to a sub-domain of the SAX-3 cytoplasmic domain (amino acids 978–1224); ActA, GST fused to the *Listeria* protein ActA. In all cases, ³⁵S-labeled probe was incubated with GST fusion proteins, coprecipitated with glutathione-agarose beads, separated by SDS-PAGE and autoradiographed.

midline axon guidance decisions. The UNC-40/DCC function is unexpected, and suggests that SAX-3/Robo and UNC-40 cooperate in a guidance process that is distinct from the known roles of UNC-40 in Netrin responses.

unc-34/Ena acts in repulsive axon guidance

unc-34 and *sax-3* both affect midline axon guidance as well as longitudinal cell migrations. In addition to these shared mutant defects, four results suggest that *unc-34* interacts with *sax-3*. First, *unc-34* mutants in double-mutant combinations have defects in AVM ventral guidance that are diagnostic of reduced SLT-1/SAX-3 activity. Second, loss of *unc-34* function suppresses SLT-1 gain of function phenotypes. Third, *unc-34* mutations enhance nerve ring defects in a weak *sax-3* mutant. Fourth, UNC-34 can bind the SAX-3 cytoplasmic domain. SAX-3 and Robo share little overall sequence similarity in their intracellular domains, but these genetic and biochemical interactions are conserved between *Drosophila* and *C. elegans*, providing strong support for their biological relevance³⁶.

The involvement of Enabled proteins in actin polymerization suggests a role for UNC-34/Enabled as an effector that links SAX-3 to the actin cytoskeleton^{43,45}. In addition, mammalian Ena-family proteins can inhibit cell motility, consistent with roles of SAX-3 in axon repulsion⁴⁶. However, our experiments do not formally distinguish whether UNC-34 acts upstream or downstream of SAX-3 (though both act downstream of SLT-1), so it is possible that UNC-34 acts as a regulator and not an effector of SAX-3.

The phenotypes of *unc-34* mutants are considerably weaker than those of *sax-3* mutants in AVM ventral guidance and in the nerve ring. Therefore, UNC-34 cannot be the sole mediator of SAX-3 activity. Evidence from *Drosophila* also suggests that additional factors, including kinases, phosphatases, *son of sevenless* and calmodulin pathways, may contribute to Robo-mediated guidance^{36,47,48}. Conversely, UNC-34 has SAX-3-independent roles in guidance. *unc-34* mutants have defects in motor neuron guidance that resemble those of *unc-5* mutants, which lack the repulsive Netrin receptor. *unc-34* also suppresses an UNC-6-dependent, UNC-5 gain-of-function axon guidance defect¹⁰. Thus *unc-34* acts in two different repulsive guidance pathways: avoidance of SLT-1 (mediated by SAX-3) and avoidance of UNC-6/Netrin (mediated by UNC-5).

Netrin-independent UNC-40 function in SAX-3 signaling

It has long been appreciated that *C. elegans unc-40* has functions that are independent of *unc-6/Netrin*^{13–16}. Our observations

UNC-34 and UNC-40 can bind SAX-3

To ask whether SAX-3, UNC-40 and UNC-34 could interact directly, we used *in vitro* binding assays to ask whether UNC-34 and UNC-40 proteins can bind SAX-3. *In-vitro* translated UNC-34 associated with a bacterially expressed GST:SAX-3 protein, but not with a GST:UNC-40 protein or with GST alone (Fig. 6a). Full-length UNC-34 also bound ActA (Fig. 6a), a *Listeria* protein that is a ligand for the EVH1 domains of vertebrate Enabled/VASP family members⁴³. UNC-34 has several unusual amino acid substitutions compared to other EVH1 domain proteins, but these results confirm that it acts as a typical ActA-binding EVH1 protein.

The UNC-40 cytoplasmic domain associated with GST:SAX-3 (Fig. 6b). This binding interaction is evolutionarily conserved, as vertebrate DCC and Robo can bind one another⁸. *In-vitro* translated UNC-40 also associated with GST:UNC-40 (Fig. 6b), consistent with observations that vertebrate DCC can dimerize⁴⁴. Similarly, *in-vitro* translated SAX-3 associated with GST:SAX-3 as well as with GST:UNC-40 (Fig. 6c). These results show that SAX-3 and UNC-40 have the potential to form homomeric and heteromeric complexes, and suggest that the observed genetic interactions could be mediated by direct interactions among SAX-3, UNC-34 and UNC-40 proteins.

DISCUSSION

Our results demonstrate that axon guidance by SAX-3, the *C. elegans* Robo protein, is potentiated by UNC-34/Enabled and UNC-40/DCC. The UNC-34/Enabled function is similar to a reported role of *Drosophila* Enabled in Robo function at the midline³⁶. Our results extend these observations to a variety of non-

demonstrate an UNC-6-independent function of UNC-40 in SAX-3 signaling. Mutations in *unc-40* but not *unc-6* suppress SLT-1 gain-of-function phenotypes in AVM and enhance weak *sax-3* loss-of-function mutations in the nerve ring. Thus, in two different cell types and two different genetic assays, UNC-40 had the properties expected of a component in the SAX-3 guidance pathway. Such a role is further supported by the direct interaction between UNC-40 and SAX-3 cytoplasmic domains.

These results suggest that SAX-3/UNC-40 complexes are required for efficient axon guidance by SAX-3. SAX-3 can mediate guidance decisions without UNC-40, just as it can without UNC-34, but in their absence SAX-3 guidance is less efficient and more sensitive to perturbation. This proposed SAX-3/UNC-40 receptor complex is analogous in some respects to the UNC-5/UNC-40 complex that acts in repulsion from Netrin. UNC-5 can mediate repulsion on its own, but efficient repulsion from Netrin requires both UNC-5 and UNC-40 (refs. 10,12,14). Thus UNC-40 can assist two repulsive receptors, SAX-3 and UNC-5, in addition to its role in Netrin attraction. Unlike UNC-5/UNC-40, however, the proposed SAX-3/UNC-40 complex crosses ligand boundaries, by linking UNC-40 to Slit responses.

An interaction between UNC-40 and SAX-3 is also observed with their vertebrate counterparts, DCC and Robo⁸, where it is implicated in a different guidance decision. In *Xenopus* spinal cord neurons, Slit acting through Robo silences the ability of DCC to mediate turning toward Netrin, but those axons are not repelled by Slit. Thus Robo can act as a negative regulator of DCC in *Xenopus* or as a collaborator with UNC-40/DCC in *C. elegans*. We speculate that the outcome of the Robo/DCC interaction is regulated by other proteins that are present or absent in particular neurons at particular developmental stages. Mouse DCC mutants have more severe defects in spinal cord axon outgrowth than do Netrin mutants, suggesting a Netrin-independent role for DCC⁴⁹; perhaps this involves an interaction with Robo proteins.

The existence of a shared guidance complex such as SAX-3/UNC-40 could help explain why there is little similarity among cytoplasmic domains of different guidance receptors. SAX-3 does not need to have the same domains as UNC-40 if it can simply recruit UNC-40 into decisions when those domains are useful. For example, a SAX-3/UNC-40 complex could promote outgrowth and motility in certain regions of the growth cone, propelling it away from a source of repellent. We suggest that local interactions between guidance receptors optimize the ability of growth cones to perform local integration of guidance cues. Turning requires the growth cone to make a decision across its surface, and during turning different regions of the growth cone behave very differently—one filopodium may be retracting as another advances. These local decisions may be best accomplished by integrating guidance decisions immediately at the level of the receptor, maximizing the interpretation of spatial information across the growth cone.

METHODS

Strains. Wild-type animals were *C. elegans* variety Bristol, strain N2. We used the following strains: CX3171 [*sax-3(ky200)* X], CX3198 [*sax-3(ky123)* X], CX5001 [*slt-1(eh15)* X], CB315 [*unc-34(e315)* V], CX4374 [*unc-34(gm104)* V], CX4345 [*unc-34(e951)* V], CX3099 [*unc-34(ky155)* V; *kyIs4* X], NW434 [*unc-6(ev400)* X], CX5353 [*unc-40(e1430)* I], CB271 [*unc-40(e271)* I], CX5088 [*zdlIs5* I; *dpy-20(e1282)* IV; *myo-3:SLT-1(kyIs213)*], CX5078 [*zdlIs5* I; *dpy-20(e1282)* IV; *myo-3:SLT-1(kyIs218)* X], CX5083 [*zdlIs5* I; *dpy-20(e1282)* IV; *myo-3:SLT-1(kyIs223)*], CX2627 [*kyIs4(ceh-23:GFP)* X], CX5334 [*oyIs14(sra-6:GFP)* V; *lin-15(n765)* X] and CX4971 [*mec-4:GFP(zdlIs5)*]. *sax-3(ky123)* deletes the start ATG and signal sequence of SAX-3. *sax-3(ky200)* encodes a P37S point mutation in the first immunoglobulin repeat¹⁷. *unc-34(gm104)* introduces an early

stop codon in the UNC-34 coding sequence. *unc-34(e951)* is a deletion that removes the EVH1 domain (M. Dell and G. Garriga, personal communication). *slt-1(eh15)* is a deletion that truncates SLT-1 after the first leucine rich repeat²⁴. *unc-6(ev400)*, *unc-40(e1430)* and *unc-40(e271)* are canonical strong loss-of-function alleles^{9,14}. Strains were maintained using standard methods. Animals were grown at 20°C except for the *sax-3(ky200)* strain, which was grown at 20°C or 25°C as noted. M. Dell and G. Garriga provided *unc-34(gm104)* and *unc-34(e951)* strains. Some strains were provided by the *Caenorhabditis* Genetic Center.

Double-mutant construction. Double mutants were constructed using standard genetic procedures. In general, *unc-34*, *unc-6* and *unc-40* were followed based on visible phenotypes, and *sax-3* and *slt-1* mutations were scored by PCR. Double Unc mutants were crossed to N2 to confirm segregation of the appropriate single mutants. *myo-3:SLT-1* homozygotes were selected based on expression of *str-1:GFP*, a marker present on the integrated *myo-3:SLT-1* array.

Characterization of neuronal phenotypes. Axons were visualized with integrated GFP transgenes and scored in live adult animals. Nerve ring sensory axons were visualized with an integrated *ceh-23:GFP* transgene (*kyIs4* X), and nerve ring interneurons were visualized with an integrated *glr-1:GFP* transgene (*kyIs29* X). The PVQ interneurons were visualized with an integrated *sra-6:GFP* transgene (*oyIs14* V, gift of Piali Sengupta). AVM axons were visualized with an integrated *mec-4:GFP* transgene (*zdlIs5*, gift of Scott Clark). Images were acquired using a Zeiss Axiocam cooled CCD or by confocal microscopy.

Isolation of the *unc-34* cDNA. A full-length *unc-34* cDNA was isolated by RT-PCR. BLAST searches identified a predicted open reading frame on chromosome V with homology to Enabled proteins. Primers were designed to the *C. elegans* trans-spliced SL1 leader sequence and to EVH1- and EVH2-related sequences of the predicted open reading frame. RT-PCR reactions with these primers yielded a 1.4 kb cDNA encoding an Enabled-related protein of 468 amino acids, with an EVH1 domain, a central proline-rich domain, and an EVH2 domain (Genbank accession number, AF535160). This sequence partially overlapped with the gene Y50D4C.1 predicted by the *C. elegans* Genome Sequencing Project. Exons 1 and 2 of *unc-34* were absent from the original Y50D4C.1 sequence and corresponded to bp 51182–51359 and 53745–54124 of the clone Y50D4C, respectively. *unc-34* exon 3 is encoded by bp 55745–55841 of Y50D4C (labelled exon 2 in Y50D4C.1). *unc-34* exon 4 is encoded by bp 58885–59306 of Y50D4C (partially overlapping predicted exon 5 of Y50D4C.1). *unc-34* exons 5, 6 and 7 correspond to bp 61574–61817, 62854–62979 and 63921–64053 of Y50D4C (exons 7, 8 and 9 of Y50D4C.1).

Cell autonomy experiments. Transgenic strains were created using standard methods. The *mec-7* promoter was used to drive expression in AVM and five other neurons (ALML/R, PLML/R, PVM)⁵⁰. For *sax-3* cell autonomy experiments, a *mec-7:SAX-3* clone²³ was injected at 50 ng/1 into *lin-15* mutants with *lin-15* and *odr-1:RFP* coinjection markers and crossed into *zdlIs5*; *sax-3(ky123)* *myo-3:SLT-1*. For *unc-34* cell autonomy experiments, the *unc-34* cDNA was cloned into the pPD96.41 *mec-7* promoter vector (gift of A. Fire and S. Xu). *mec-7:unc-34* was injected at 50 ng/1 into *lin-15* mutants with *lin-15* and *odr-1:RFP* and crossed into *zdlIs5*; *unc-34(e951)*; *myo-3:SLT-1*. A *mec-7:UNC-40* construct was provided by J. Culotti⁹. For *unc-40* cell autonomy experiments, *mec-7:UNC-40* was injected at 10 ng/1 with *odr-1:RFP* into *zdlIs5* *unc-40(e1430)*; *myo-3:SLT-1*. Transgenic strains were analyzed for rescue of AVM phenotypes, with non array-bearing siblings serving as controls.

Generation of proteins for binding analysis. Expression vectors for *in vitro* translation of SAX-3, UNC-40 and UNC-34 probes were constructed in pCITE-4c (Novagen, Madison, Wisconsin). The following clones were generated: CITE:SAX-3(898–1273), CITE:UNC-40(1106–1415) and CITE:UNC-34(1–467). These were used to generate 35[S]-methionine-labeled probes by *in vitro* transcription/translation (TNT T7 Quick Coupled Transcription/Translation kit, Promega, Madison, Wisconsin). Expression vectors for GST-fusion proteins were constructed in pGEX-4T-1 (Amersham, Piscataway, New Jersey). The

following GST-fusion proteins were produced: GST:SAX-3(898–1273), GST:SAX-3(978–1224), GST:UNC-40(1106–1415) and GST:ActA. GST-fusions were expressed in *E. coli* BL21-CodonPlus RIL (Stratagene, La Jolla, California), purified using glutathione agarose beads (Sigma), and quantitated by SDS-PAGE and Coomassie staining. For binding assays, 2 µg of GST fusion protein was mixed with 20 µl of 35[S]-methionine-labeled probe in 10 mM Tris 7.5, 150 mM NaCl, 0.1% Triton and 0.05% BSA. Samples were incubated for six hours at 4°C and then washed three times in the same buffer. BSA was omitted from the last wash. Bound proteins were separated by SDS-PAGE, soaked in Amplify (Amersham), dried down under vacuum and exposed to film.

Acknowledgments

We thank K. Prehoda, D. Lee, J. Zallen, S. Clark and Z. Gitai for discussions and ideas that facilitated this work, M. Dell and G. Garriga for communicating results before publication, S. Clark, P. Sengupta, A. Fire and J. Culotti for clones and strains, and C. Adler, T. Saxton, S. Shaham and E. Stein for comments on the manuscript. T.W.Y. was supported by a MIND Institute predoctoral fellowship and the UCSF MSTP. J.C.H. was supported by an HHMI predoctoral fellowship. C.I.B. and M.T.L. are Investigators of the Howard Hughes Medical Institute. This work was supported by the Howard Hughes Medical Institute.

Competing interests statement

The authors declare that they have no competing financial interests.

RECEIVED 6 AUGUST; ACCEPTED 11 SEPTEMBER 2002

1. Tessier-Lavigne, M. & Goodman, C. S. The molecular biology of axon guidance. *Science* 274, 1123–1133 (1996).
2. Culotti, J. G. & Merz, D. C. DCC and netrins. *Curr. Opin. Cell Biol.* 10, 609–613 (1998).
3. Flanagan, J. G. & Van Vactor, D. Through the looking glass: axon guidance at the midline choice point. *Cell* 92, 429–432 (1998).
4. Brose, K. & Tessier-Lavigne, M. Slit proteins: key regulators of axon guidance, axonal branching, and cell migration. *Curr. Opin. Neurobiol.* 10, 95–102 (2000).
5. Flanagan, J. G. & Vanderhaeghen, P. The ephrins and Eph receptors in neural development. *Annu. Rev. Neurosci.* 21, 309–345 (1998).
6. Nakamura, F., Kalb, R. G. & Strittmatter, S. M. Molecular basis of semaphorin-mediated axon guidance. *J. Neurobiol.* 44, 219–229 (2000).
7. Bashaw, G. J. & Goodman, C. S. Chimeric axon guidance receptors: the cytoplasmic domains of slit and netrin receptors specify attraction versus repulsion. *Cell* 97, 917–926 (1999).
8. Stein, E. & Tessier-Lavigne, M. Hierarchical organization of guidance receptors: silencing of netrin attraction by slit through a Robo/DCC receptor complex. *Science* 291, 1928–1938 (2001).
9. Chan, S. S. *et al.* UNC-40, a *C. elegans* homolog of DCC (Deleted in Colorectal Cancer), is required in motile cells responding to UNC-6 netrin cues. *Cell* 87, 187–195 (1996).
10. Colavita, A. & Culotti, J. G. Suppressors of ectopic UNC-5 growth cone steering identify eight genes involved in axon guidance in *Caenorhabditis elegans*. *Dev. Biol.* 194, 72–85 (1998).
11. Hamelin, M., Zhou, Y., Su, M. W., Scott, I. M. & Culotti, J. G. Expression of the UNC-5 guidance receptor in the touch neurons of *C. elegans* steers their axons dorsally. *Nature* 364, 327–330 (1993).
12. Hong, K. *et al.* A ligand-gated association between cytoplasmic domains of UNC5 and DCC family receptors converts netrin-induced growth cone attraction to repulsion. *Cell* 97, 927–941 (1999).
13. Hedgecock, E. M., Culotti, J. G., Hall, D. H. & Stern, B. D. Genetics of cell and axon migrations in *Caenorhabditis elegans*. *Development* 100, 365–382 (1987).
14. Hedgecock, E. M., Culotti, J. G. & Hall, D. H. The *unc-5*, *unc-6*, and *unc-40* genes guide circumferential migrations of pioneer axons and mesodermal cells on the epidermis in *C. elegans*. *Neuron* 4, 61–85 (1990).
15. Kim, S., Ren, X. C., Fox, E. & Wadsworth, W. G. SDQR migrations in *Caenorhabditis elegans* are controlled by multiple guidance cues and changing responses to netrin UNC-6. *Development* 126, 3881–3890 (1999).
16. Honigberg, L. & Kenyon, C. Establishment of left/right asymmetry in neuroblast migration by UNC-40/DCC, UNC-73/Trio and DPY-19 proteins in *C. elegans*. *Development* 127, 4655–4668 (2000).
17. Zallen, J. A., Yi, B. A. & Bargmann, C. I. The conserved immunoglobulin superfamily member SAX-3/Robo directs multiple aspects of axon guidance in *C. elegans*. *Cell* 92, 217–227 (1998).
18. Kidd, T. *et al.* Roundabout controls axon crossing of the CNS midline and defines a novel subfamily of evolutionarily conserved guidance receptors. *Cell* 92, 205–215 (1998).

19. Tear, G., Seeger, M. & Goodman, C. S. To cross or not to cross: a genetic analysis of guidance at the midline. *Perspect. Dev. Neurobiol.* 1, 183–194 (1993).
20. Kidd, T., Russell, C., Goodman, C. S. & Tear, G. Dosage-sensitive and complementary functions of *roundabout* and *commissureless* control axon crossing of the CNS midline. *Neuron* 20, 25–33 (1998).
21. Guthrie, S. Axon guidance: Robos make the rules. *Curr. Biol.* 11, R300–303 (2001).
22. Kidd, T., Bland, K. S. & Goodman, C. S. Slit is the midline repellent for the robo receptor in *Drosophila*. *Cell* 96, 785–794 (1999).
23. Zallen, J. A., Kirch, S. A. & Bargmann, C. I. Genes required for axon pathfinding and extension in the *C. elegans* nerve ring. *Development* 126, 3679–3692 (1999).
24. Hao, J. C. *et al.* *C. elegans* Slit acts in midline, dorsal-ventral, and anterior-posterior guidance via the SAX-3/Robo receptor. *Neuron* 32, 25–38 (2001).
25. Brose, K. *et al.* Slit proteins bind Robo receptors and have an evolutionarily conserved role in repulsive axon guidance. *Cell* 96, 795–806 (1999).
26. Zou, Y., Stoeckli, E., Chen, H. & Tessier-Lavigne, M. Squeezing axons out of the gray matter: a role for slit and semaphorin proteins from midline and ventral spinal cord. *Cell* 102, 363–375 (2000).
27. Fricke, C., Lee, J. S., Geiger-Rudolph, S., Bonhoeffer, F. & Chien, C. B. *astray*, a zebrafish *roundabout* homolog required for retinal axon guidance. *Science* 292, 507–510 (2001).
28. Bagri, A. *et al.* Slit proteins prevent midline crossing and determine the dorsoventral position of major axonal pathways in the mammalian forebrain. *Neuron* 33, 233–248 (2002).
29. Plump, A. S. *et al.* *Slit1* and *Slit2* cooperate to prevent premature midline crossing of retinal axons in the mouse visual system. *Neuron* 33, 219–232 (2002).
30. Gallo, G. & Letourneau, P. C. Axon guidance: a balance of signals sets axons on the right track. *Curr. Biol.* 9, R490–R492 (1999).
31. Merz, D. C. & Culotti, J. G. Genetic analysis of growth cone migrations in *Caenorhabditis elegans*. *J. Neurobiol.* 44, 281–288 (2000).
32. Lin, M. Z. & Greenberg, M. E. Orchestral maneuvers in the axon: trio and the control of axon guidance. *Cell* 101, 239–242 (2000).
33. Gertler, F. B., Doctor, J. S. & Hoffmann, F. M. Genetic suppression of mutations in the *Drosophila abl* proto-oncogene homolog. *Science* 248, 857–860 (1990).
34. Gertler, F. B. *et al.* *enabled*, a dosage-sensitive suppressor of mutations in the *Drosophila Abl* tyrosine kinase, encodes an Abl substrate with SH3 domain-binding properties. *Genes and Development* 9, 521–533 (1995).
35. Wills, Z., Bateman, J., Korey, C. A., Comer, A. & Van Vactor, D. The tyrosine kinase Abl and its substrate enabled collaborate with the receptor phosphatase Dlar to control motor axon guidance. *Neuron* 22, 301–312 (1999).
36. Bashaw, G. J., Kidd, T., Murray, D., Pawson, T. & Goodman, C. S. Repulsive axon guidance: Abelson and Enabled play opposing roles downstream of the roundabout receptor. *Cell* 101, 703–715 (2000).
37. Fire, A. *et al.* Potent and specific genetic interference by double-stranded RNA in *Caenorhabditis elegans*. *Nature* 391, 806–811 (1998).
38. Forrester, W. C. & Garriga, G. Genes necessary for *C. elegans* cell and growth cone migrations. *Development* 124, 1831–1843 (1997).
39. McIntire, S. L., Garriga, G., White, J., Jacobson, D. & Horvitz, H. R. Genes necessary for directed axonal elongation or fasciculation in *C. elegans*. *Neuron* 8, 307–322 (1992).
40. White, J. G., Southgate, E., Thomson, J. N. & Brenner, S. The structure of the nervous system of the nematode *Caenorhabditis elegans*. *Phil. Trans. R. Soc. Lond. B Biol. Sci.* 314, 1–340 (1986).
41. Wadsworth, W. G., Bhatt, H. & Hedgecock, E. M. Neuroglia and pioneer neurons express UNC-6 to provide global and local netrin cues for guiding migrations in *C. elegans*. *Neuron* 16, 35–46 (1996).
42. Hiramoto, M., Hiromi, Y., Giniger, E. & Hotta, Y. The *Drosophila* Netrin receptor Frazzled guides axons by controlling Netrin distribution. *Nature* 406, 886–889 (2000).
43. Chakraborty, T. *et al.* A focal adhesion factor directly linking intracellularly motile *Listeria monocytogenes* and *Listeria ivanovii* to the actin-based cytoskeleton of mammalian cells. *EMBO J.* 14, 1314–1321 (1995).
44. Stein, E., Zou, Y., Poo, M. & Tessier-Lavigne, M. Binding of DCC by netrin-1 to mediate axon guidance independent of adenosine A2B receptor activation. *Science* 291, 1976–1982 (2001).
45. Laurent, V. *et al.* Role of proteins of the Ena/VASP family in actin-based motility of *Listeria monocytogenes*. *J. Cell Biol.* 144, 1245–1258 (1999).
46. Bear, J. E. *et al.* Negative regulation of fibroblast motility by Ena/VASP proteins. *Cell* 101, 717–728 (2000).
47. Sun, Q., Bahri, S., Schmid, A., Chia, W. & Zinn, K. Receptor tyrosine phosphatases regulate axon guidance across the midline of the *Drosophila* embryo. *Development* 127, 801–812 (2000).
48. Fritz, J. L. & VanBerkum, M. F. Calmodulin and *son of sevenless* dependent signaling pathways regulate midline crossing of axons in the *Drosophila* CNS. *Development* 127, 1991–2000 (2000).
49. Fazeli, A. *et al.* Phenotype of mice lacking functional *Deleted in colorectal cancer* (*Dcc*) gene. *Nature* 386, 796–804 (1997).
50. Hamelin, M., Scott, I. M., Way, J. C. & Culotti, J. G. The *mec-7* beta-tubulin gene of *Caenorhabditis elegans* is expressed primarily in the touch receptor neurons. *EMBO J.* 11, 2885–2893 (1992).

